

Supplementary Materials for
Age-dependent acquisition of pathogenicity by SARS-CoV-2 Omicron BA.5

Brian Imbiakha *et al.*

Corresponding author: Hector C. Aguilar, ha363@cornell.edu; Avery August, averyaugust@cornell.edu

Sci. Adv. **9**, eadj1736 (2023)
DOI: 10.1126/sciadv.adj1736

This PDF file includes:

Figs. S1 to S5
Table S1

Supplemental Figure 1

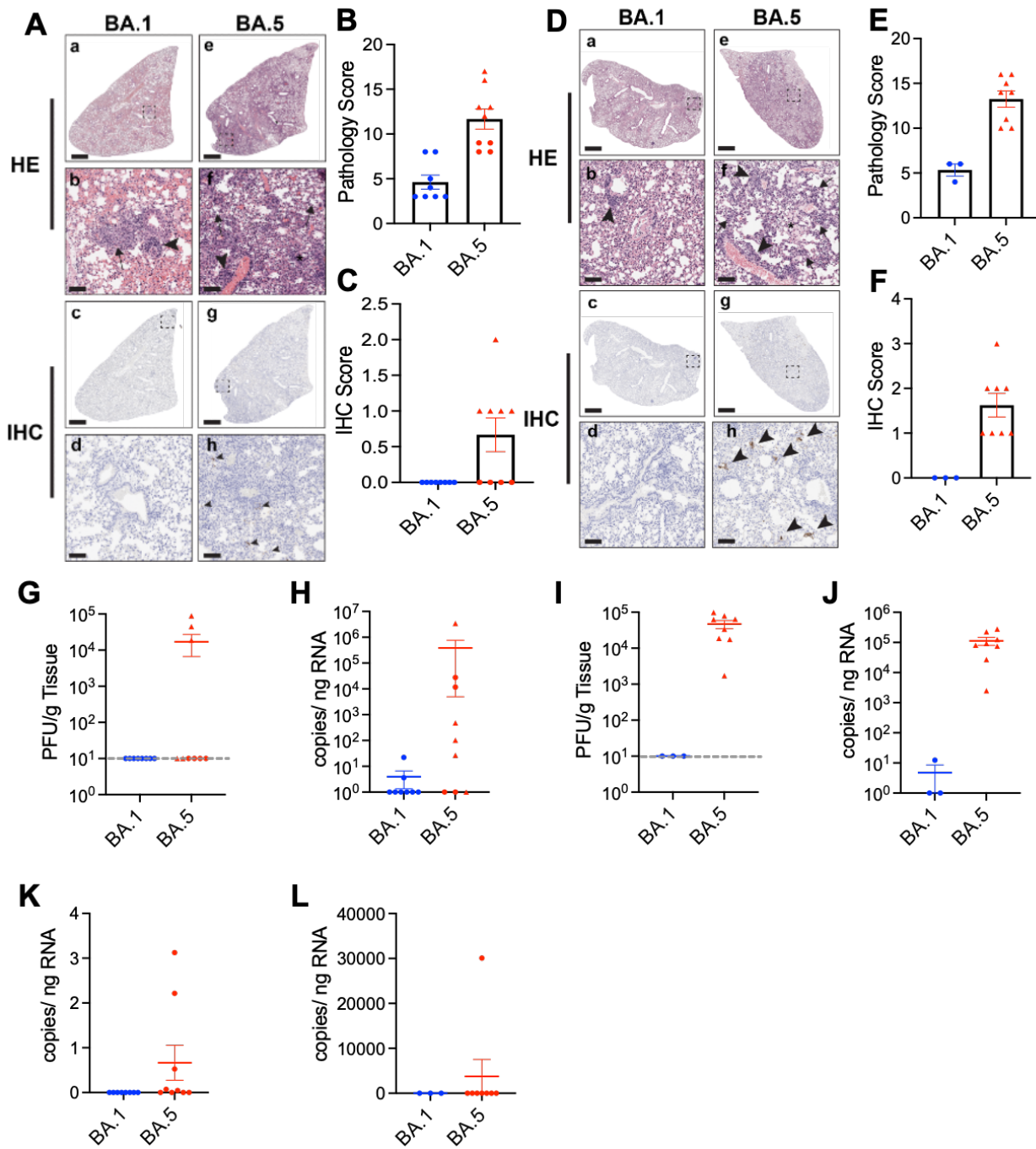


Figure S1: SARS-CoV-2 Omicron BA.5 induces increased virus titers and pathology following infection. A-F. K18-hACE2 mice were infected with 3.25×10^4 PFU SARS-CoV-2 Omicron BA.1 and BA.5. Lungs were collected for H&E and IHC. A. Representative H&E staining (a,b,e,f) of lung histopathology or IHC for SARS-CoV-2 N protein (c,d,g,h) (one section analyzed per mouse) in Omicron BA.1 infected 3 month old mice at 14 dpi (a-d) or Omicron BA.5 (e-h) (BA.1 n = 8, BA.5 n = 9). Mice infected with Omicron BA.5 had more significant lesions with increased perivascular infiltrates (arrowheads), interstitial infiltrates (asterisk), inflammatory cells in alveoli (arrow), and mild alveolar edema compared to mice infected with Omicron BA.1. Scale bar a,c,e,g = 1 mm ; b,d,f,h = 100 μ m. For histopathology and IHC analyses, representative images were selected based on the mean pathological score. B. Histopathology scores at death or endpoint. Triangle represents mice euthanized before 14 dpi and circle represent mice euthanized 14 dpi (BA.1 n = 8, BA.5 n = 9). C. IHC score at death or endpoint. Triangles represent mice euthanized before 14 dpi and circles represent mice euthanized 14 dpi (BA.1 n = 8, BA.5 n = 9).

before 14 dpi and circles represent mice euthanized 14 dpi (BA.1 $n = 8$, BA.5 $n = 9$). **D.** Representative H&E staining (a,b,e,f) of lung histopathology or IHC staining with an anti-SARS-CoV-2 N protein antibody (c,d,g,h) (one section analyzed per mouse) at 14 dpi in 5-8 month old mice infected with Omicron BA.1 (a-d) or Omicron BA.5 (e-h) (BA.1 $n = 3$, BA.5 $n = 8$). Mice infected with Omicron BA.5 had more significant lesions with increased perivascular infiltrates (arrowheads), interstitial infiltrates (arrows), edema in alveoli (asterisk), and inflammatory cells in alveoli compared to mice infected with Omicron BA.1. Scale bar a,c,e,g = 1 mm ; b,d,f,h = 100 μm . For histopathology and IHC analyses, representative images were selected based on the mean pathological score. **E.** Histopathological score at death or endpoint. Triangle represents mice euthanized before 14 dpi and circle represent mice euthanized 14 dpi (BA.1 $n = 3$, BA.5 $n = 8$). **F.** IHC scores at death or endpoint. Triangles represent mice euthanized before 14 dpi and circles represent mice euthanized 14 dpi (BA.1 $n = 3$, BA.5 $n = 8$). Data are means \pm S.E.M. **G.** Virus titers in the lungs of 3-month old mice (BA.1 $n = 8$, BA.5 $n = 9$). Triangles represent mice euthanized before 14 dpi and circles represent mice euthanized 14 dpi. Data are means \pm S.E.M. **H.** Viral RNA in the lungs of 3-month old mice at endpoint (BA.1 $n = 8$, BA.5 $n = 9$). Data are means \pm S.E.M. **I.** Virus titers in the lungs of 5-8 month old mice (BA.1 $n = 3$, BA.5 $n = 8$). Data are means \pm S.E.M. **J.** Viral RNA levels in the lung of 5-8 month old mice (BA.1 $n = 3$, BA.5 $n = 8$). Data are means \pm S.E.M. **K.** Viral RNA in the brains of 3-month old mice at endpoint (BA.1 $n = 8$, BA.5 $n = 9$). Data are means \pm S.E.M. **L.** Viral RNA in the brains of 5-8 month old mice at endpoint (BA.1 $n = 3$, BA.5 $n = 8$). Data are means \pm S.E.M.

Supplemental Figure 2

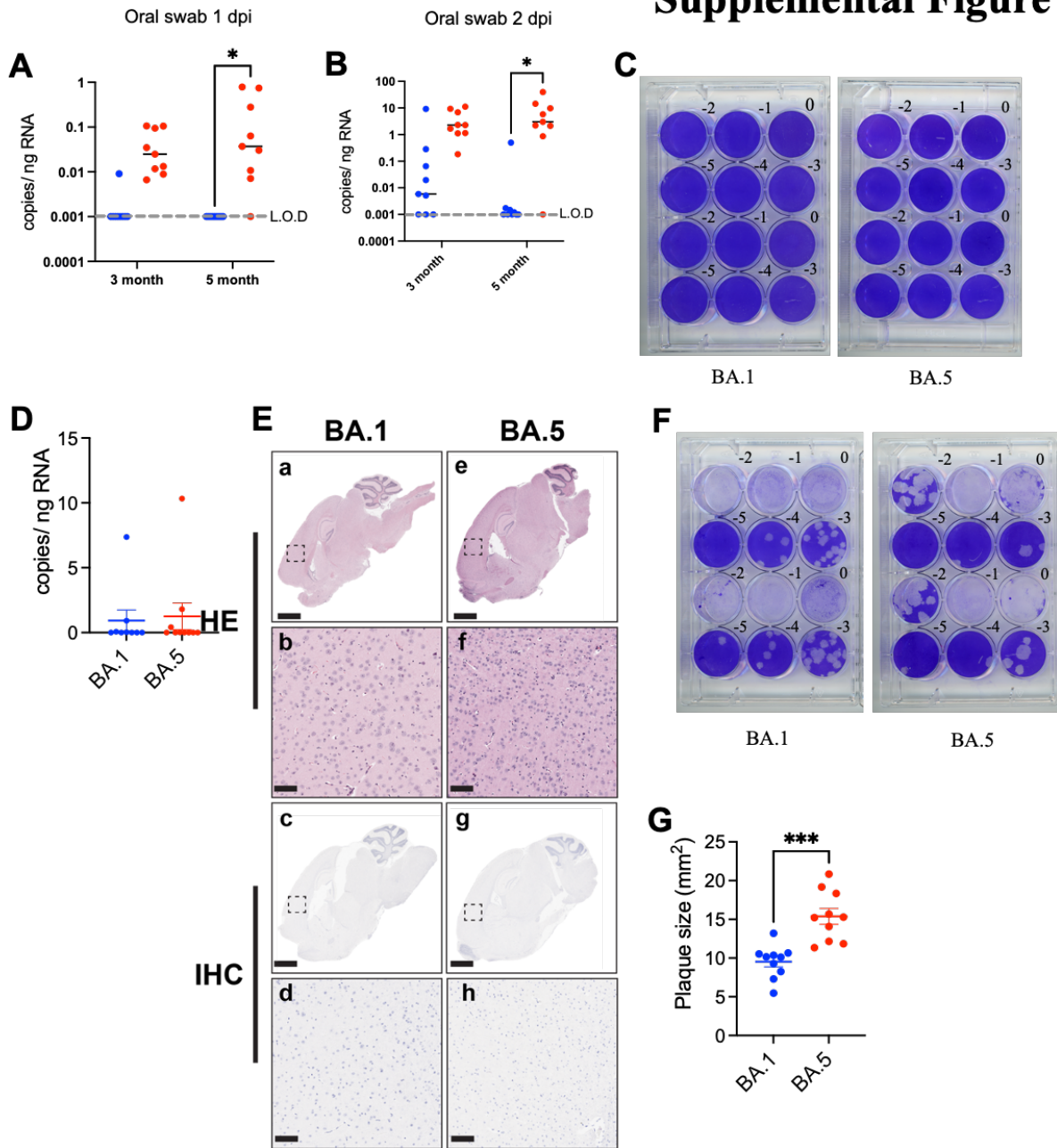
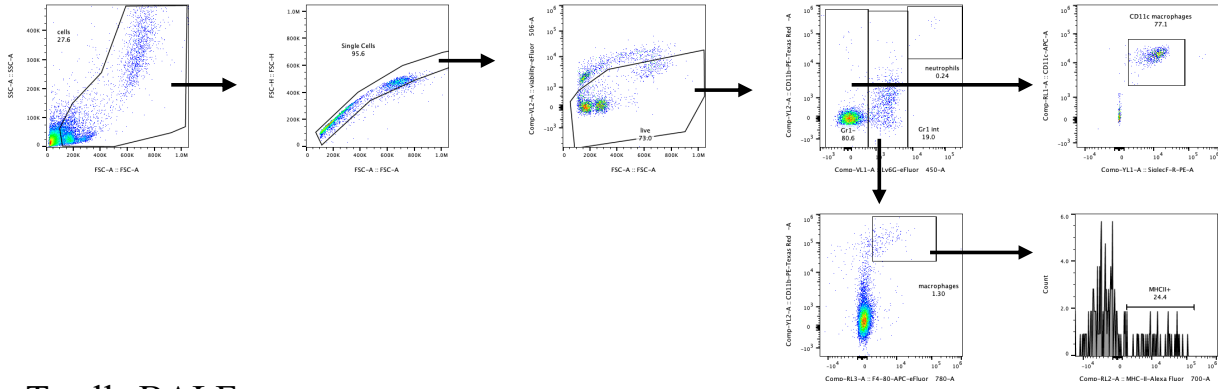


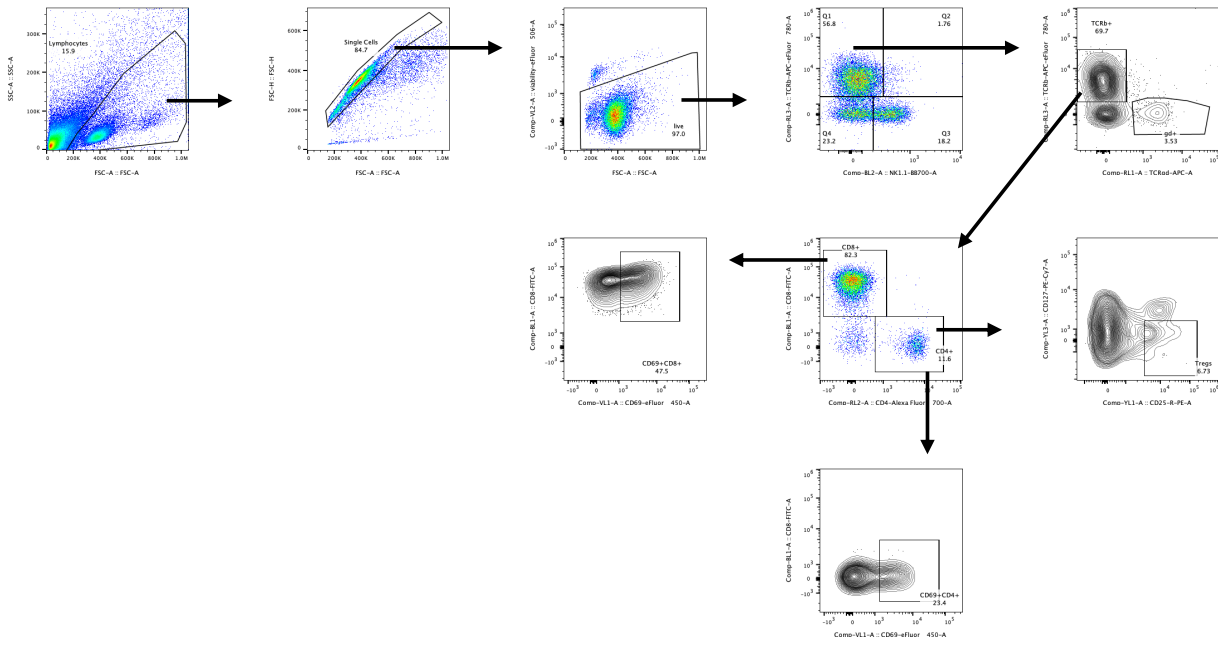
Figure S2: Viral titers 1, 2 and 5 dpi. **A.** Viral RNA quantification by RT-qPCR in the oral cavity of 3 and 5 month old K18-hACE2 mice infected with Omicron BA.1 and Omicron BA.5 (BA.1 $n = 9$, BA.5 $n = 9$) at 1 dpi, or **B.** 2 dpi. **C.** Brain plaques from 2 dpi. **D.** Brain viral RNA quantification by RT-qPCR from 5 dpi (BA.1 $n = 9$, BA.5 $n = 10$). **E.** Representative H&E staining (a,b,e,f) or IHC staining with an anti-SARS-CoV-2 N protein antibody (c,d,g,h) (one section analyzed per mouse) of brain tissue at death or study endpoint in K18-hACE2 mice infected with Omicron BA.1 (a-d) or Omicron BA.5 (e-h). The brain of all mice infected with either strain is histologically normal with no evidence of immunolabeling. Scale bar a,c,e,g = 2 mm ; b,d,f,h = 100 μ m. **F.** Lung plaques, and **G.** Lung plaque area from 5 dpi (BA.1 $n = 10$, BA.5 $n = 10$). One-way ANOVA with Tukey's multiple comparison test.

Supplemental Figure 3

Granulocytes BALF



T cells BALF



B cells

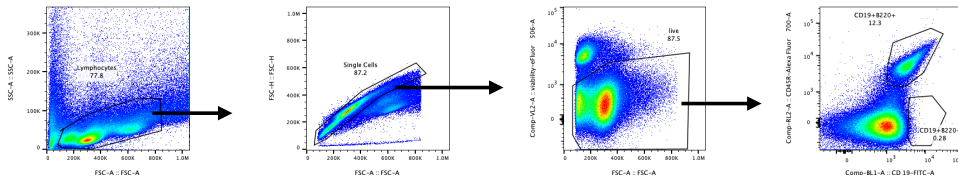


Figure S3: Gating strategy for analysis of lung immune cells. Cells were stained and analyzed via flow cytometry. Representative images are shown to demonstrate the gating strategy for the indicated populations.

Supplemental Figure 4

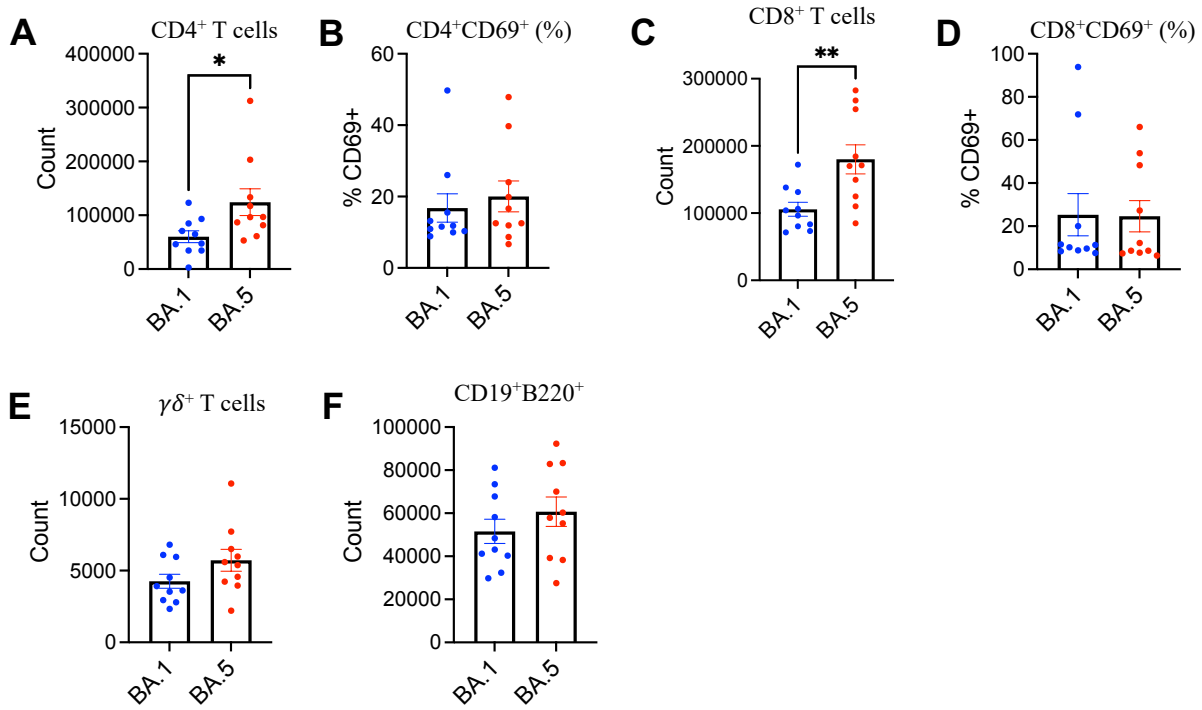


Figure S4: Lymph node immune cell profile following SARS-CoV-2 Omicron infection. K18-hACE2 mice were infected with SARS-CoV-2 Omicron BA.1 and BA.5 (BA.1 $n = 10$, BA.5 $n = 10$). At 5 dpi, mediastinal lymph nodes were collected and immune cells were analyzed by flow cytometry. **A.** Total CD4⁺ cells in the lymph nodes. **B.** Percent activated CD4⁺ T cells. **C.** CD8⁺ T cells in the lymph node. **D.** Percent activated CD8⁺ T cells. **E.** $\gamma\delta$ T cells in the lymph node. **F.** Total B cells in the lymph node. All data are means \pm S.E.M.

Supplemental Figure 5

	-----NTD-----	
Omicron BA.5	MFVFLVLLPLVSSQCVNLITRTQ---SYTNSFTRGVVYPDKVFRSSVLHSTQDLFLPFFS	57
Omicron BA.1	MFVFLVLLPLVSSQCVNLTRTQLPPAYTNSFTRGVVYPDKVFRSSVLHSTQDLFLPFFS	60
Wuhan-Hu-1	MFVFLVLLPLVSSQCVNLTRTQLPPAYTNSFTRGVVYPDKVFRSSVLHSTQDLFLPFFS	60

Omicron BA.5	NVTWFHAI--SGTNGIKRFDNPVLPFNDGVYFASTEKSNIIRGWIFGTTLDSKTQSLIV	115
Omicron BA.1	NVTWFHVI--SGTNGTKRFDNPVLPFNDGVYFASIEKSNIIRGWIFGTTLDSKTQSLIV	118
Wuhan-Hu-1	NVTWFHAIHVSGTNGTKRFDNPVLPFNDGVYFASTEKSNIIRGWIFGTTLDSKTQSLIV	120

Omicron BA.5	NNATNVVIKVFCEFCNDPFLDVYYHKNNKSWMESEFRVYSSANNCTFEYVSQPFLMDLE	175
Omicron BA.1	NNATNVVIKVFCEFCNDPFLDVYYHKNNKSWMESEFRVYSSANNCTFEYVSQPFLMDLE	178
Wuhan-Hu-1	NNATNVVIKVFCEFCNDPFLGVYYHKNNKSWMESEFRVYSSANNCTFEYVSQPFLMDLE	180

Omicron BA.5	GKQGNFKNLRFEVFKNIDGYFKIYSKHTPIINL--GRDLPQGFSALEPLVDLPIGINITRF	233
Omicron BA.1	GKQGNFKNLRFEVFKNIDGYFKIYSKHTPIIVREPEDLPQGFSALEPLVDLPIGINITRF	238
Wuhan-Hu-1	GKQGNFKNLRFEVFKNIDGYFKIYSKHTPIINL--VRDLPQGFSALEPLVDLPIGINITRF	238

Omicron BA.5	QTLALHRSYLT PGDSSSGWTAGAAAYVGYLQPRTFLLKYNENGTITDAVDCALDPLSE	293
Omicron BA.1	QTLALHRSYLT PGDSSSGWTAGAAAYVGYLQPRTFLLKYNENGTITDAVDCALDPLSE	298
Wuhan-Hu-1	QTLALHRSYLT PGDSSSGWTAGAAAYVGYLQPRTFLLKYNENGTITDAVDCALDPLSE	298

Omicron BA.5	TKCTLKSFVTEKGIYQTSNFRVQPTESIVRFPNITNLCPFDEVFNATRFASVYAWNRKRI	353
Omicron BA.1	TKCTLKSFVTEKGIYQTSNFRVQPTESIVRFPNITNLCPFDEVFNATRFASVYAWNRKRI	358
Wuhan-Hu-1	TKCTLKSFVTEKGIYQTSNFRVQPTESIVRFPNITNLCPFGEVFNATRFASVYAWNRKRI	358
-----RBD-----		
Omicron BA.5	SNCVADYSVLYNFAPFFAFKCYGVSPTKLNLDLCFTNVYADSFVIRGNEVSIAPGQTGNI	413
Omicron BA.1	SNCVADYSVLYNLAPFFTFCYGVSPKLNLDLCFTNVYADSFVIRGDEVRIAPGQTGNI	418
Wuhan-Hu-1	SNCVADYSVLYNSASFSTFKCYGVSPTKLNLDLCFTNVYADSFVIRGDEVRIAPGQTGKI	418

Omicron BA.5	ADYNYKLPDDFTGCVIAWNSNKLDSKVGNYNYRRLFRKSNLKPFFERDISTEIIYQAGNK	473
Omicron BA.1	ADYNYKLPDDFTGCVIAWNSNKLDSKVSIGNYNYLYRRLFRKSNLKPFFERDISTEIIYQAGNK	478
Wuhan-Hu-1	ADYNYKLPDDFTGCVIAWNSNKLDSKVGNYNYLYRRLFRKSNLKPFFERDISTEIIYQAGST	478

Omicron BA.5	PCNGVAGVNCYFPLQSYGFRPTYGVGHQPYRVVLSFELLHAPATVCGPKKSTNLVKNKC	533
Omicron BA.1	PCNGVAGVNCYFPLRSYSFRPTYGVGHQPYRVVLSFELLHAPATVCGPKKSTNLVKNKC	538
Wuhan-Hu-1	PCNGVEGFNCYFPLQSYGFQPTNGVGYQPYRVVLSFELLHAPATVCGPKKSTNLVKNKC	538

Omicron BA.5	VNFNFNGLTGTGVLTESNKKFLPFQFGRDIADTTDAVRDPQTEIILDITPCSFGGVSVI	593
Omicron BA.1	VNFNFNGLKGTGVLTESNKKFLPFQFGRDIADTTDAVRDPQTEIILDITPCSFGGVSVI	598
Wuhan-Hu-1	VNFNFNGLTGTGVLTESNKKFLPFQFGRDIADTTDAVRDPQTEIILDITPCSFGGVSVI	598

Omicron BA.5	TPGTNTSNQVAVLYQGVNCTEVPVAIHADQLTPTRVYSTGNSVVFQTRAGCLIGAEYVNN	653
Omicron BA.1	TPGTNTSNQVAVLYQGVNCTEVPVAIHADQLTPTRVYSTGNSVVFQTRAGCLIGAEYVNN	658
Wuhan-Hu-1	TPGTNTSNQVAVLYQDVNCTEVPVAIHADQLTPTRVYSTGNSVVFQTRAGCLIGAEHVNN	658

	S1/S2	
Omicron BA.5	SYECDIPIGAGICASYQTQTKSHRRARSVASQSI IAYTMSLGAENSVAYSNNSIAIPTNF	713
Omicron BA.1	SYECDIPIGAGICASYQTQTKSHRRARSVASQSI IAYTMSLGAENSVAYSNNSIAIPTNF	718
Wuhan-Hu-1	SYECDIPIGAGICASYQTQTNSPRRARSVASQSI IAYTMSLGAENSVAYSNNSIAIPTNF	718

Omicron BA.5	TISVTEILPVSMTKTSVDCTMYICGDSTEC SNLLQYGSFCTQLKRALTGI AVEQDKNT	773
Omicron BA.1	TISVTEILPVSMTKTSVDCTMYICGDSTEC SNLLQYGSFCTQLKRALTGI AVEQDKNT	778
Wuhan-Hu-1	TISVTEILPVSMTKTSVDCTMYICGDSTEC SNLLQYGSFCTQLNRALTGI AVEQDKNT	778

S2' --fusion peptide----

Omicron BA.5	QEVFAQVKQIYKTPPIKYFGGFNFSQILPDPSKPSKRSFIEDLLFNKVTLADAGFIKQYG	833
Omicron BA.1	QEVFAQVKQIYKTPPIKYFGGFNFSQILPDPSKPSKRSFIEDLLFNKVTLADAGFIKQYG	838
Wuhan-Hu-1	QEVFAQVKQIYKTPPIKDFGGFNFSQILPDPSKPSKRSFIEDLLFNKVTLADAGFIKQYG	838

Omicron BA.5	DCLGDIAARDLICAQKFNGLTVLPPLLTDEMQIAQYTSALLAGTITSGWTFGAGAALQIPF	893
Omicron BA.1	DCLGDIAARDLICAQKFGKGLTVLPPLLTDEMQIAQYTSALLAGTITSGWTFGAGAALQIPF	898
Wuhan-Hu-1	DCLGDIAARDLICAQKFNGLTVLPPLLTDEMQIAQYTSALLAGTITSGWTFGAGAALQIPF	898
-----HR1-----		
Omicron BA.5	AMQMAYRFNGIGVTVQNVLYENQKLIANQFNLSAIGKIQDSLSTASALGKLDVNVHNAQA	953
Omicron BA.1	AMQMAYRFNGIGVTVQNVLYENQKLIANQFNLSAIGKIQDSLSTASALGKLDVNVHNAQA	958
Wuhan-Hu-1	AMQMAYRFNGIGVTVQNVLYENQKLIANQFNLSAIGKIQDSLSTASALGKLDVNVQNAQA	958
-----HR2-----		
Omicron BA.5	LNTLVKQLSSKFGAISSVLNDILSRDLKVEAEVQIDRLITGRLQSLQTYVTTQQLIRAAEI	1013
Omicron BA.1	LNTLVKQLSSKFGAISSVLNDIFSRDLKVEAEVQIDRLITGRLQSLQTYVTTQQLIRAAEI	1018
Wuhan-Hu-1	LNTLVKQLSSNFGAISSVLNDILSRDLKVEAEVQIDRLITGRLQSLQTYVTTQQLIRAAEI	1018
-----TM-----		
Omicron BA.5	RASANLAATKMSECVLGQSKRVDFCGKGYHLMSFPQSAPHGVVFLHVTYVPAQEKNFTTA	1073
Omicron BA.1	RASANLAATKMSECVLGQSKRVDFCGKGYHLMSFPQSAPHGVVFLHVTYVPAQEKNFTTA	1078
Wuhan-Hu-1	RASANLAATKMSECVLGQSKRVDFCGKGYHLMSFPQSAPHGVVFLHVTYVPAQEKNFTTA	1078

Omicron BA.5	PAICHDGKAHFPRGCVFVSNNGTHWFVTVQRNFYEPQIITTDNTFVSGNCDVVIQVNNVTY	1133
Omicron BA.1	PAICHDGKAHFPRGCVFVSNNGTHWFVTVQRNFYEPQIITTDNTFVSGNCDVVIQVNNVTY	1138
Wuhan-Hu-1	PAICHDGKAHFPRGCVFVSNNGTHWFVTVQRNFYEPQIITTDNTFVSGNCDVVIQVNNVTY	1138

Omicron BA.5	DPLQPELDSFKEELDKYFKNHTSPDVLGDISGINASVVNIQKEIDRLNEVAKNLNESLI	1193
Omicron BA.1	DPLQPELDSFKEELDKYFKNHTSPDVLGDISGINASVVNIQKEIDRLNEVAKNLNESLI	1198
Wuhan-Hu-1	DPLQPELDSFKEELDKYFKNHTSPDVLGDISGINASVVNIQKEIDRLNEVAKNLNESLI	1198
-----CT-----		
Omicron BA.5	DLQELGKYEQYIKWPWYIWLGFIAGLIAIVMVTIMLCCMTSCCSCLKGCSCGSCCKFDE	1253
Omicron BA.1	DLQELGKYEQYIKWPWYIWLGFIAGLIAIVMVTIMLCCMTSCCSCLKGCSCGSCCKFDE	1258
Wuhan-Hu-1	DLQELGKYEQYIKWPWYIWLGFIAGLIAIVMVTIMLCCMTSCCSCLKGCSCGSCCKFDE	1258

Omicron BA.5	DDSEPVKGVKLYHT*	1269
Omicron BA.1	DDSEPVKGVKLYHT*	1274
Wuhan-Hu-1	DDSEPVKGVKLYHT*	1274

Figure S5: Sequence alignment of SARS-CoV-2 S proteins comparing SARS-CoV-2 Wuhan to Omicron BA.1 and Omicron BA.5.

Supplemental Table 1

Supplemental Table 1		
Cell Markers	Fluorochrome	Manufacturer and Catalog#
CD8	fitc	invitrogen 11-0081-85
NK1.1	BB700	BD BioSciences 566503
CD25	PE	invitrogen 12-0251-83
KLRG1	pe-TexasRed	BD BioSciences 565393
CD127	PE-Cy7	invitrogen 25-1271-82
TCRgd	APC	BioLegend 118116
CD4	AF700	invitrogen 56-0041-82
TCRb	APC-cy7	BioLegend 109220
CD69	Pacific Blue	BioLegend 104524
CD62L	Pac Orange	BioLegend 104433
CD19	fitc	invitrogen 11-0193-85
IgG2a, IgG2b	BB700	BD Biosciences 745969
CD138	PE	invitrogen MA5-23527
IgM	PE-ef610	invitrogen 61-5790-82
CD23	PE-Cy7	invitrogen 25-0232-82
Fas	APC	invitrogen 17-0951-82
CD45R (B220)	AF700	invitrogen 56-0452-82
CD27	APC-AF780	invitrogen 47-0271-82
GL7	ef450	invitrogen 48-5902-82
IgD	SB600	invitrogen 63-5993-82
c-kit	Fitc	BD BioSciences 553354
CD69	BB700	BD BioSciences 566501
Siglec F	PE	BD BioSciences 552126
CD11b	PE-Dazzle594	BioLegend 101256
CD49b	PECy7	BioLegend 103518
CD11c	APC	BioLegend 117310
MHCII	AF700	invitrogen 56-5321-80
F4/80	APC-Cy7	BioLegend 123118
Ly6G	Pacific Blue	BioLegend 127612
viability	ef506	invitrogen 65-0866-14
CD16/32	---	invitrogen 14-0161-85

Flow cytometry antibodies.